

Oxidation behaviour of Zn nanoclusters

A. K. Mahapatra* and T. Som

Institute of Physics, Sachivalaya Marg, Bhubaneswar 751005, India

Zn nanoclusters are deposited by Low energy cluster beam deposition technique. The morphology, composition and structure of deposited nanoclusters are analyzed, after exposing to the ambient, by high resolution transmission electron microscopy. It is observed that Zn nanoclusters are converted to Zn-ZnO (core-shell), Zn-void-ZnO or hollow ZnO type nanoclusters, depending upon their size, by reacting with oxygen present in the ambient. Nanoclusters bigger than ~ 15 nm are of Zn-ZnO (core-shell) type. Among them, nanoclusters between ~ 15 to 25 nm are of irregular or distorted geometrical shaped, and above ~ 25 nm are of geometrical shaped (viz. triangular, hexagonal, rectangular and rhombohedral). It is reasoned, the external shape of nanocluster is related to its internal atomic arrangements. ZnO is in epitaxial relationship with the underlying Zn surface. Nanoclusters between ~ 15 to 5 nm are observed to be Zn-void-ZnO type, and smaller than ~ 5 nm are perfect ZnO hollow sphere type, i.e. ZnO hollow nanoclusters. The observed oxidation behaviour of nanoclusters are compared with theory of Cabrera-Mott (CM) on low temperature oxidation of metal. It is argued that CM theory is based on simple assumptions and can not explain oxidation behaviour of nanometals satisfactorily. However, in agreement with CM theory, the oxide layer after reaching certain critical thickness able to protect the nanometal from further degradation.

INTRODUCTION

The future generation devices will use a lot of nanometer size metals in them. Nanomaterials have a large surface to volume ratio. Also, enthalpy of oxide formation for many metals is low [1]. Hence, nanometals easily get oxidized, even in a high vacuum environment. Functioning and life time of devices could be significantly altered if its nanometal components get oxidized. Therefore, studying oxidation behaviour of metals of nanometer size has technological importance. It can also be noted that metal-oxide (metal-semiconductor) interfaces have been playing a key role in many micro-electronics and optoelectronic applications [2]. Hence fabrication of metal-oxide interface in nanometer scale by simple process of oxidation in a controlled manner could be very helpful in technological application as well as for fundamental study.

Oxidation process on bulk metal surfaces is being studied extensively for a century. The process of oxidation, at low temperature, is generally believed to follow in accordance to the mechanism proposed by Cabrera and Mott (CM). In CM theory [3], it is assumed that a layer of atomic oxygen get adsorbed on a metal surface when it is exposed to atmosphere. Electrons from metal can tunnel through the initial oxide layers and ionize the adsorbed oxygen atoms. It results in setting up a potential difference across the oxide layer. The potential difference lowers the activation energy required for metal ions to diffuse and helps in increasing the oxide thickness at oxide-gas interface. The growth rate of oxide is very high up to a certain limiting thickness, after which, it becomes too low that an increase in oxide thickness practically stops. So at constant temperature, thin uniform layer of oxide forms over a metal surface and protects the metal from further degradation. Quantitative calculations based on

CM theory give oxide thickness of around 2-3 nm for most of the metals at room temperature. Understanding on the subject is still limited due to lack of confirmatory experimental verification. In recent papers [4–6], validity of some basic assumptions made in the CM theory are examined by carrying out advanced experimental techniques. High resolution transmission electron microscopy (HRTEM) is one such advanced technique, which could be very helpful in understanding oxidation behaviour of metal, by analyzing the structure and morphology of oxide layer.

It should be noted that CM theory deals with oxidation behaviour of a bulk metal surface, which is flat. But in a nanocluster, number of faces are more than one and corners are also involved in the oxidation process. In addition, physical and chemical properties of the material change as it reduces to nanometer range [7]. In a bulk metal, thickness of oxide is insignificantly small compared to the metal. But in case of nanoclusters, thickness of oxide layer, which is formed by consuming metal atoms, is comparable to size of the original metal core. Hence, it is necessary to examine the suitability of CM theory to explain oxidation behaviour of nanometals.

In this paper, we are reporting oxidation behaviour of Zn nanoclusters by analyzing their morphology, composition, and structure. Zn nanoclusters are directly deposited on to the carbon coated transmission electron microscope (TEM) Cu-grid by low energy cluster beam deposition (LECBD) technique and analyzed by HRTEM. The observations are compared with CM theory. It is argued that Cabrera-Mott theory is based on simple assumptions and can not explain oxidation behaviour of nanometals satisfactorily. It is observed that Zn nanoclusters are converted to Zn-ZnO (core-shell), Zn-void-ZnO or ZnO hollow sphere type, depending upon their size, by reacting with oxygen present in the ambient.

Nanoclusters bigger than ~ 15 nm are Zn-ZnO core-shell type and between ~ 15 to 5 nm are Zn-void-ZnO type. Nanoclusters smaller than ~ 5 nm are ZnO hollow spheres. Bigger size nanoclusters above ~ 25 nm are geometrical shaped, mainly triangular, hexagonal, rectangular and rhombohedral. Zn-ZnO core-shell nanoclusters ranging from size ~ 15 to 25 nm are of irregular or distorted geometrical shapes. Probable reason for the observed shape is given.

LECBD technique is chosen to make initial Zn nanostructures instead of other techniques because it has many advantages which is suitable for this specific study. In LECBD technique, the main advantage is nanoclusters form through homogeneous nucleation in contrast to most of the synthesis process. Effect of substrate on shape is insignificant as nanoclusters first form in vacuum environment and then deposit on substrate in a soft landing process. Therefore, shape of nanocrystals purely depends on the intrinsic characteristics of the material. Also, it was possible to deposit well separated nanocrystals with varied but well-defined geometrical shapes in a single run. Therefore, oxidation behaviour could be studied for varied shape and size by analyzing each nanoclusters independently. High-purity zinc powder and argon gas are used to avoid effect of impurities on the oxidation behaviour. Otherwise, this could complicate the study and lead to poor reproducibility. Hence, modification in composition and morphology of initial nanoclusters can be assigned solely to the interaction of Zn nanoclusters with the ambient atmosphere.

EXPERIMENTAL

Nanocluster deposition process can be considered as a three step process: (i) Formation of Zn atomic vapours, (ii) homogeneous nucleation and growth of nanoclusters in an argon gas atmosphere, and (iii) extraction (from growth region) and deposition of nanoclusters on the substrate. The cluster generating source used for the present study is of Sattler type [8]. Zn vapours are formed by heating Zn powder using resistive coil in a molybdenum crucible at 740 K. Zn vapours come out of the crucible through a hole that is present in the side wall. A carrier gas (viz. argon) continuously flows into the condensation chamber and gets out through a tubular outlet to the vacuum chamber. This tubular outlet is kept at a low temperature by circulating liquid nitrogen (LN_2) around it. Zn monomers transfer their energy to LN_2 -cooled inert gas atoms and achieve supersaturation [9]. This results in homogeneous nucleation and growth of Zn nanoclusters. The cluster generating source and substrates are kept in a vacuum chamber where pressure maintained at $\sim 10^{-6}$ mbar. Passage of gas leads to a rise in the chamber pressure to $\sim 10^{-4}$ mbar. Thermophoretic force [10] originating from temperature gradient between

the hot crucible and the LN_2 -cooled tubular outlet, and force due to pressure gradient help nanoclusters to come out of the gas condensation chamber through the tubular outlet. Nanoclusters coming out of the tubular outlet undergo an adiabatic expansion which leads to further reduction in their temperature. Since nanoclusters go through successive stages of cooling, they have very low kinetic energy and get deposited on the substrate without fragmentation. Details of the LECBD set-up has been reported elsewhere [11]. Silicon wafer attached with TEM grid are used as the substrate. After deposition, flow of argon gas and LN_2 are stopped. Pressure of chamber again comes back to $\sim 10^{-6}$ mbar after stopping flow of argon gas and this condition is maintained for around 10 hours. During this time, temperature of the crucible slowly cooled down to room temperature. Then chamber pressure is maintained at $\sim 10^{-3}$ mbar for another one day before breaking vacuum of the chamber. Grid-case containing TEM grids, are preserved inside an air-tight box. After 10 days and again after 3 months, the grids are used for TEM study.

RESULTS AND DISCUSSIONS

Typical TEM micrographs of deposited nanoclusters are shown in Fig. 1. The projected area diameter of several nanoclusters are measured and number of nanoclusters counted per each size range is plotted in Fig. 1b. A Gaussian distribution with an average size of 20.7 nm and standard deviation of 15.7 nm best fits to the data points. Selected area electron diffraction (SAED) pattern of nanoclusters are shown in the inset of Fig. 1a. Arrangement of diffraction spots in form of a discrete ring pattern suggests a polycrystalline nature of the sample. Inter-planar spacings (d -spacings) are calculated from the diffraction pattern and are in good agreement with those of (002) and (101) planes of Zn [12].

A contrast between ZnO shell (lighter contrast) and Zn core (darker contrast) of the nanoclusters is observed in TEM micrographs when viewed with higher magnification (marked by arrows in Fig. 1c). Contrast between core and the shell region becomes more prominent with further magnification. Zn-ZnO core-shell structure of a single nanocluster is shown in the inset of Fig. 1c. HRTEM (Fig. 2a) validates the formation of Zn-ZnO (core-shell) nanocluster. ZnO (shell) region is marked in the figure and thickness measured to be around 3.0 nm. The fast Fourier transform (FFT) pattern of shell region (rectangular outline (\bar{a})) is shown in Fig. 2b. The spots are indexed corresponding to hexagonal crystal structure (space group= $P6_3mc$) having lattice parameters $a=0.324$ nm and $c=0.5206$ nm [13]. The spots correspond to (100) family of lattice planes along the [001] zone axis. By filtering the FFT spot patterns, the original HRTEM of region (a) in Fig. 2a is reconstructed and is shown

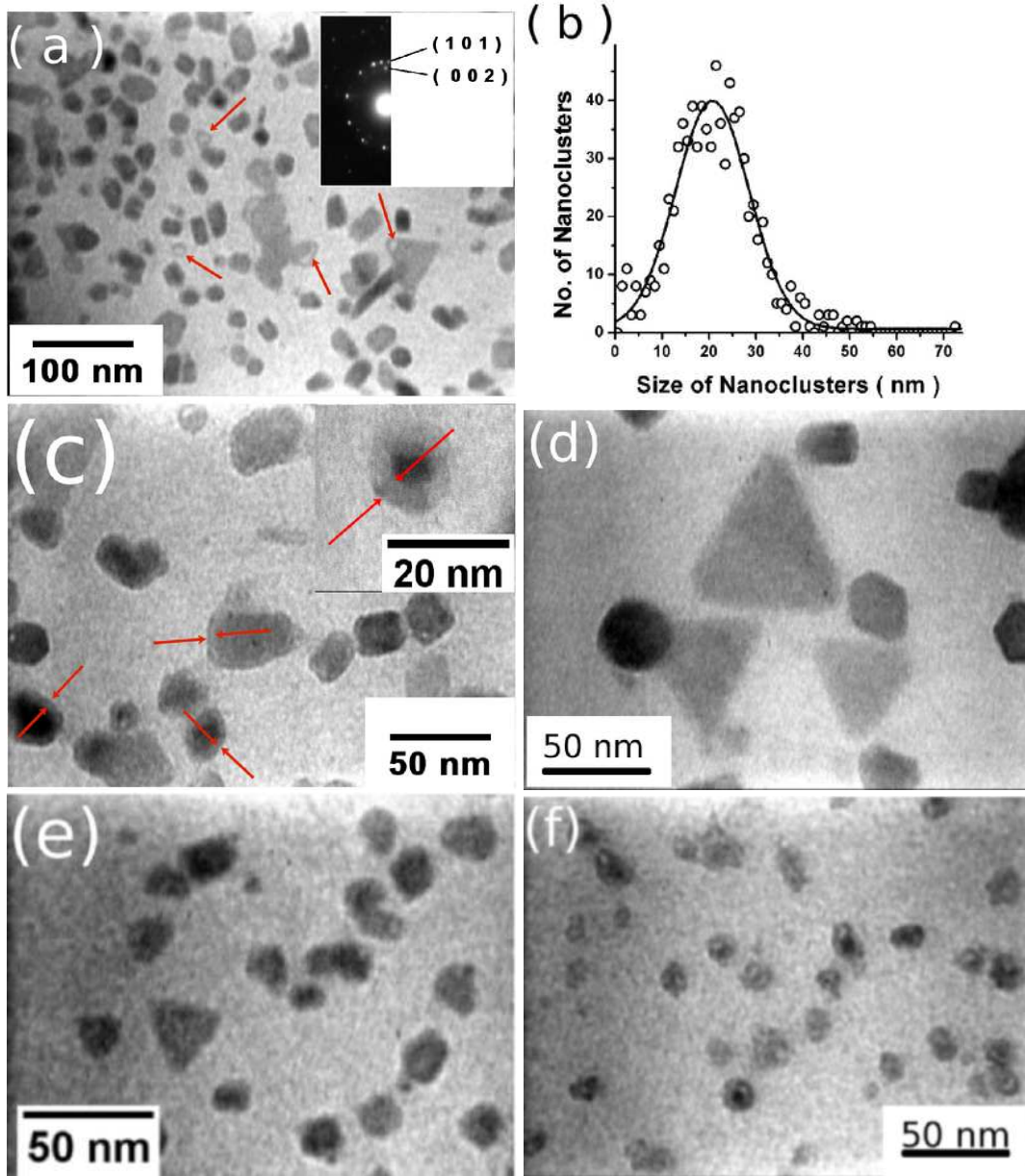


FIG. 1. Typical TEM micrographs of Zn/ZnO nanoclusters: (a) Arrow marks highlight the presence of voids in the nanoclusters (SAED pattern is shown in the inset), (b) size distribution of nanoclusters, (c) nanoclusters of different size group, where arrow mark shows the ZnO shell with a lighter contrast. A single Zn-ZnO core-shell nanocluster, at a higher magnification, is shown in the inset, (d) geometrical shaped nanoclusters of average size larger than ~ 25 nm, (e) irregular or distorted geometrical shaped nanoclusters of size ~ 25 to 15 nm, and (f) Zn-void-ZnO type nanoclusters of size ~ 15 to 5 nm

in Fig. 2d. The d -spacing of 0.28 nm is obtained from the line profile study (Fig. 2f), which corresponds to the (100) planes of ZnO. The HRTEM image shown here is a portion of a hexagonal shaped Zn-ZnO (Core-shell) nanocluster. The Zn nanocluster is faceted with (100) planes over which ZnO (100) plane grows epitaxially. This results in observation of Moiré pattern in core region as d -value of Zn and ZnO are different (rectangular outline (b) in Fig. 2a). FFT of the region clearly shows that the spots correspond to (100) planes of ZnO and Zn along the [001] zone axis (marked by arrows in Fig. 2c) and also suggests $(100)_{\text{Zn}} // (100)_{\text{ZnO}}$ epitaxial relationship [14].

To highlight the Moiré fringes, the spots marked with arrows in FFT, are filtered and the HRTEM image is reconstructed (Fig. 2e). The line profile is plotted in Fig. 2g. It may be noticed that in each Moiré repeat six planes of ZnO are present and the spacing between Moiré repeat is 1.6 nm. If d_{shell} and d_{core} are the inter-planar spacings of the shell and the core regions then spacing between the Moiré fringes will be $D = d_{\text{shell}}d_{\text{core}}/(d_{\text{shell}} - d_{\text{core}})$ and the number of planes in a Moiré repeat is given by $n = d_{\text{shell}}/(d_{\text{shell}} - d_{\text{core}})$. By putting d -spacing of (100) planes of both Zn and ZnO in the above equation $D = 1.3$ nm and $n = 5.6$ is obtained, which is consistent with

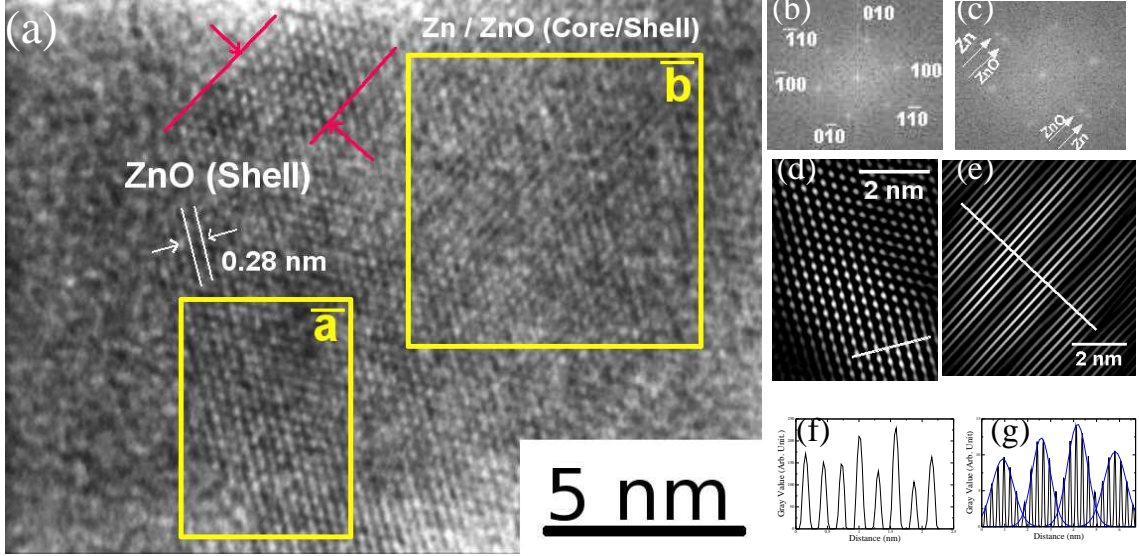


FIG. 2. (a) Typical HRTEM image of a hexagonal shaped Zn-ZnO core-shell nanocluster, (b) FFT pattern of the shell region, that is outlined by a rectangle \bar{a} in fig.(a), (c) FFT pattern of the core region, that is outlined by rectangle \bar{b} in fig.(a), (d) reconstructed HRTEM image after filtering the FFT spot patterns of fig.(b), (e) reconstructed HRTEM image after filtering the FFT spot patterns, marked with arrows, of fig.(c), (f) gray value along the line drawn in fig. (d), and (g) gray value along the line drawn in fig. (e)

the observed value.

The enthalpy of oxide formation is quite low for zinc [1]. So zinc oxidizes easily when it comes in contact with oxygen. As per the CM theory, oxide thickness increases according to the following growth rate:

$$\frac{dX}{dt} = N' \Omega \nu \exp\left(\frac{qa'V}{kTX} - \frac{W}{kT}\right) \quad (1)$$

Symbol has the same meaning as in Ref. [3]. To compare experimental results with CM theory, an attempt has been made to estimate limiting thickness of the oxide shell by taking standard values of parameters available in the literature [15]: $a'=0.25$ nm, $q=+2e$, $N' = 1.6 \times 10^{15}$ atoms/cm², $\Omega = 2.3 \times 10^{-23}$ cm³/atom, $\nu = 4.3 \times 10^{12}$ sec⁻¹. At room temperature, the value of kT can be taken as 0.025 eV. The value of V can be approximated to $\frac{-\Delta G(ZnO)}{2e}$, where ΔG is the free energy for formation of the oxide per oxygen atom [16]. Taking $\Delta G(ZnO) = -318.2$ kJ mol⁻¹, potential difference developed across the thin film (V) will be 1.65 Volt. The value of W can be approximated to the activation energy of the metal tracer diffusion coefficient in the oxide and is taken as 1.8 eV [17]. Putting these values in Eq. (1), it can be seen that at oxide thickness of 1.1 nm the growth rate becomes 0.1 nm per day and finally reduces to 0.1 nm per year corresponding to an oxide thickness of 1.3 nm only. It means the thickness of ZnO shell is expected to be ≤ 1.3 nm. However, oxide shell thickness even up to 5 nm is observed in some nanoclusters, which is much larger than the value estimated from Eq. (1). Nakamura

et al. also observed a ZnO shell thickness of 4 nm at room temperature [18].

The observed oxide shell thickness is much larger than the estimated value possibly due to following reasons: (i) When size of a material reduces to nanometer range, electronic property of the material changes. Hence, value of V , basically the difference in metal Fermi level and O^- level, would be different than the one used in the equation. In principle, value of V will be different from one nanocluster to the other, depending on its shape and size. (ii) In CM theory, it is assumed that oxygen ion can not diffuse through the initial oxide layer due to its higher diffusion co-efficient. Metal ions can only diffuse. So that oxide layer can only grow at the metal-gas interface, not at the metal-oxide interface. However, it is observed that in some metals oxygen diffuses through the initial oxide layer and reacts with metal ions. Fehler and Mott (FM) later on expanded the CM theory by introducing the possibility of oxygen to diffuse and contribute to the growth of oxide [19]. As per FM theory, rate of oxygen diffusion depends on structure of the initial oxide layer. If density of easy diffusion paths like grain boundaries or dislocations are high enough in the initial oxide layer then diffusion of both metal as well as oxygen ions contribute to the oxide growth. In the present study, HRTEM of deposited Zn-ZnO (core-shell) nanoclusters show presence of dislocations at the interface. HRTEM image of the interface, having dislocations, is shown in Fig. 3a. In order to show the presence of dislocations in a clear manner, the HRTEM is reconstructed by filtering the FFT pattern (Fig. 3b). It is seen that at every five or six (100)

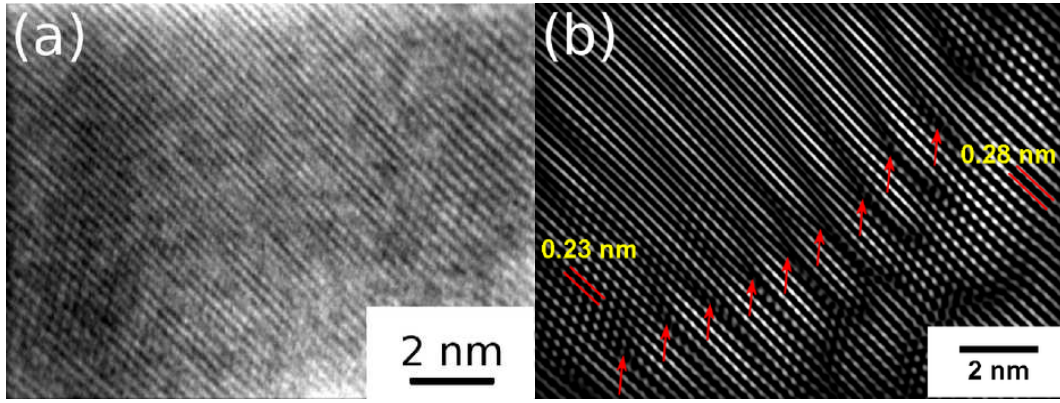


FIG. 3. (a) HRTEM of interface showing presence of dislocations, (b) reconstructed image after filtering FFT pattern of HRTEM of Fig.(a)

planes there is a misfit dislocation (shown by arrows). The inter-planar spacings of 0.23 nm and 0.28 nm, that is written in the figure, correspond to d -values of (100) planes of Zn and ZnO, respectively. However, presence of dislocations resulted in observation of irregular Moiré fringes and fluctuation in the d -value due to lattice contraction and relaxation. Some experimental studies on oxidation behaviour of bulk Cu surfaces [5, 6] show that oxide film does not grow in a uniform layer-by-layer fashion as assumed in CM theory, but instead, separate oxide islands nucleate which then grow laterally, coalesce with each other and form a thin layer over the metal surface. The process of lateral growth and coalescence of oxide islands result in formation of grain boundaries. Similar mechanism might be happening during oxidation of Zn surfaces. Thus, in oxidation process of Zn nanoclusters, diffusion of reactant ions through grain boundaries and dislocations might have dominated over the bulk diffusion. So value of W could be much less than the one used in the Eq. (1), and oxygen diffusion could have contributed significantly towards an increase in the oxide thickness. Increase in oxide thickness by both oxygen and metal ion diffusion is also proposed for Fe nanoparticles [20].

HRTEM shown in Fig. 2 and Fig. 3 are portion of big size nanoclusters (above ~ 25 nm). The big size nanoclusters (Fig. 1d) are observed to be of geometrical shapes (viz. rectangular, rhombohedral, triangular, and hexagonal). Shape of a crystal, grown in laboratory, depends on two factors [21]: (i) The internal factors (bonding strength and symmetries of atomic arrangements) and (ii) the external factors (growth parameters and conditions). The way monomers supplied around a growing crystal and the nature of foreign atoms present in the environment are two major external factors. Most of the crystal growth procedures used to prepare nanoclusters do not have control over these two external factors. Therefore, original intrinsic shape of nanocluster gener-

ally get modified. In LECBD technique, however, clusters during their growth get uniform supply of monomers around them as they travel along the tubular outlet. In addition, influence of foreign atoms is avoided as clusters are grown in a vacuum condition by using high purity materials. Thus, shape of nanoclusters mainly depend on internal factors. The symmetries displayed by the external shape of nanocluster is actually symmetries of its internal atomic arrangements. Zn belongs to the hexagonal crystal system. Point group of hexagonal crystal system has all the symmetry elements that rhombohedral, orthorhombic, monoclinic, triclinic system have. So, deposited nanoclusters are of hexagonal, rhombohedral, orthorhombic, monoclinic, and triclinic shape. Since in TEM micrographs only two-dimensional projection of the object can be seen, observed shape of a nanocluster is also related to its orientation with respect to the electron beam.

However, nanoclusters below ~ 25 nm are not of geometrical shapes. It is mainly due to effect of oxidation. A small size nanocluster has more facets compared to big one. Since, surface energies and lattice constants of Zn and ZnO are different for different faces, density of grain boundaries and dislocations is not same for all. It results a wide variation in growth rate and thickness of oxide for different faces of crystal [22, 23], and primarily responsible for distortion of the original shape. Noticeable change in shape is not observed for big size nanoclusters because they have less number of facets compared to small size nanoclusters, and also ratio of newly formed oxide shell thickness to original core size is small. Observation of irregular or distorted geometrical shaped nanoclusters is prominent for nanoclusters of size ~ 25 to 15 nm (Fig. 1e). Nanoclusters below ~ 15 nm, in addition being irregularly shaped, are different in structure and composition. Unlike being core-shell structure, nanoclusters between ~ 15 to 5 nm are of Zn-void-ZnO type and smaller than that are perfect ZnO hollow sphere type, i.e ZnO hollow

nanoclusters.

Although diffusion of both zinc and oxygen ions contribute to growth of oxide, their rates of diffusion are not same. Outward diffusion of zinc is comparatively much higher than the inward diffusion of oxygen, which results in accumulation of vacancies inside the metal. When concentration of vacancies becomes higher than its equilibrium concentration, stable void forms [24]. It is noteworthy to mention here that vacancies diffuse much more rapidly than atoms in a material. So distribution of vacancies inside a material is generally uniform [25]. Therefore, in nanoclusters bigger than ~ 15 nm, concentration of vacancies is not sufficient to develop supersaturation and form voids. Only in corners of some big nanoclusters, voids are formed as a result of local supersaturation, due to higher vacancy generation rate compared to its diffusion during early stage of oxidation. For nanoclusters of size ~ 15 to 5 nm, all Zn metal could not converted to ZnO. So remaining amount of Zn remains in the core, with a cap-like void and a shell of ZnO around it (Fig. 1f). However, for nanoclusters below ~ 5 nm, all Zn atoms are consumed and perfect ZnO hollow nanoclusters are formed. It should be noted that formation of void due to material loss is also not taken into account in CM theory. The hollow ZnO nanoclusters, Zn-void-ZnO type nanoclusters and a big nanocluster with a void in the corner are shown by arrow marks in Fig. 1a. After three months of exposure to the ambient, the samples were re-examined. It was observed that morphology and composition of nanoclusters did not change significantly. It is in agreement with the CM theory that oxide, after certain limiting thickness, will passivate the surface and protect the metal from further loss.

CONCLUSIONS

Zn nanoclusters are deposited by LECBD technique. The morphology, composition and structure of deposited nanoclusters are analyzed by HRTEM after exposing to the ambient. It is argued that Cabrera-Mott theory is based on simple assumptions and can not explain oxidation behaviour of nanometals satisfactorily. A better theory is needed to explain the oxidation behaviour of nanometals. However, in agreement with CM theory the oxide layer after reaching certain thickness are able to protect the nanometal from further degradation. Zn nanoclusters are converted to Zn-ZnO (core-shell) type, Zn-void-ZnO type or hollow ZnO nanoclusters by reacting with oxygen present in the ambient. The final morphology is dependent on the initial shape and size of the deposited Zn nanocluster. Nanoclusters bigger than ~ 15 nm are of Zn-ZnO (core-shell) type. Among them, ~ 15 to 25 nm nanoclusters are of irregular or distorted geometrical shaped. But, nanoclusters above ~ 25 nm are geometrical shaped. Shape of the nanoclusters is re-

lated to symmetry of the internal atomic arrangements. Significant modification in shape due to oxidation is not observed for these big size nanoclusters. It is also observed that, the oxide grows in epitaxial relationship with underlying Zn surface. Nanoclusters ~ 15 to 5 nm are Zn-void-ZnO type and smaller than ~ 5 nm are perfect hollow ZnO nanoclusters. Voids are formed due to higher outward diffusion of Zn compared to inner diffusion of oxygen.

ACKNOWLEDGEMENT

The help received from Prof. S. N. Sahu, Dr. S. N. Sarangi, and Mr. G. Swain for carrying out experiment in LECBD set - up is gratefully acknowledged. The help received from Prof. P. V. Satyam and Mr. A. K. Dash in doing the TEM measurement is also gratefully acknowledged. The encouragement received from Prof. S. R. Bhattacharyya, Saha Institute of Nuclear Physics, Kolkata is gratefully acknowledged.

* Present address:

Saha Institute of Nuclear Physics, 1/AF, Bidhan Nagar, Kolkata - 700064, India

Email addresses :

amulya@iopb.res.in (A. K. Mahapatra)

tsom@iopb.res.in (T. Som)

- [1] C. T. Campbell; *Surf. Sci. Rep.*, **27**, 1 (1997)
- [2] Sze SM; *Physics of semiconductor devices*. Wiley Interscience (1981)
- [3] N. Cabrera, N. F. Mott; *Rep. Prog. Phys.*, **12**, 163 (1949)
- [4] K. Thürmer, E. Williams, J. R. Robey, *Science*, **297**, 2033 (2002)
- [5] G. Zhou, J. C. Yang; *Phys. Rev. Lett.*, **89**, 106101 (2002)
- [6] J. C. Yang, B. Kolasa, J. M. Gibson, M. Yeadon; *Appl. Phys. Lett.*, **73**, 2841 (1998)
- [7] A. K. Mahapatra; *J. Nanopart. res.*, **11**, 467 (2009)
- [8] K. Sattler, J. Mühlbach, E. Recknagel; *Phys. Rev. Lett.*, **45**, 821 (1980)
- [9] H. Min, W. Zhaoye, C. Pingping, Y. Shengwen, W. Guanghou; *Nucl. Instr. and Meth. in Phys. Res. B*, **135**, 564 (1998)
- [10] P. Han, T. Yoshida; *J. Appl. Phys.*, **91**, 1814 (2002)
- [11] G. V. R. Prasad, B. K. Patel, S. Chakravarty, R. Mythili, M. Vijaylakshmi, B. R. Sekhar, S. N. Sahu, V. S. R. Ramamurthy, S. N. Behera; *Current Science*, **80**, 280 (2001)
- [12] Joint Committee on Powder Diffraction Standards (JCPDS), File no. 04-0831.
- [13] Joint Committee on Powder Diffraction Standards (JCPDS), File no. 36-1451
- [14] Y. Ding, X. Y. Kong, Z. L. Wang; *J. Appl. Phys.*, **95**, 306 (2004)

- [15] D. R. Lide; *CRC handbook of chemistry and physics*, CRC Press, Inc., 71st edition (1990)
- [16] A. Atkinson; *Rev. of Mod. Phys.*, **57**, 437 (1985)
- [17] B. J. Wuensch, H. L. Tuller; *J. Phys. Chem. Solids*, **55**, 975 (1994)
- [18] R. Nakamura, J. G. Lee, D. Tokozakura, H. Mori, H. Nakajima; *Materials letters*, **61**, 1060 (2007)
- [19] F. P. Fehlner, N. F. Mott; *Oxidation of Metals*, **2**, 59 (1970)
- [20] C. M. Wang, D. R. Baer, L. E. Thomas, J. E. Amonette, J. Antony, Y. Qiang, G. Duscher; *J. Appl. Phys.*, **98**, 094308 (2005)
- [21] X. Y. Liu, P. Bennema; *Phys. Rev. B*, **49**, 765 (1994)
- [22] J. V. Cathcart, G. F. Petersen, C. J. Sparks; *J. Electrochem. Soc.*, **116**, 664 (1969)
- [23] K. R. Lawless; *Rep. Prog. Phys.*, **37**, 231 (1974)
- [24] M. Bobeth, M. Gutkin, W. Pompe, A. E. Romanov; *Phys. Stat. Sol. (a)*, **165**, 165 (1998)
- [25] K. A. Jackson; *Kinetic Processes*, WILEY-VCH Verlag GmbH & Co. KGaA. (2004)